AIAA JOURNAL
Vol. 43, No. 9, September 2005

Flow Simulation Around an Airfoil by Lattice Boltzmann Method on Generalized Coordinates

Taro Imamura*
Japan Aerospace Exploration Agency, Tokyo 182-8522, Japan
Kojiro Suzuki†
Tokyo University, Tokyo 113-0033, Japan
and
Takashi Nakamura‡ and Masahiro Yoshida§
Japan Aerospace Exploration Agency, Tokyo 182-8522, Japan

Flow simulations around an airfoil (NACA0012) using the lattice Boltzmann method (LBM) are performed. Originally, the LBM is an incompressible flow solver on orthogonal coordinates. However, to resolve the boundary layer of the airfoil accurately, the algorithm is extended to generalized coordinates. Also, a suitable wall boundary condition is introduced for generalized coordinates. First, the numerical method is validated at a relatively small Reynolds number ($Re = 500$). The velocity profile of the boundary layer is compared in detail with the computational fluid dynamics code CFL3D (developed at NASA Langley Research Center) results, and consistent results are obtained. Second, the method is combined with the Baldwin–Lomax turbulence model and results at relatively high Reynolds number ($Re = 5 \times 10^5$) are shown. The results are in good agreement with the experimental data. With the same grid resolution, the method can solve high-Reynolds-number flows as accurately as traditional Navier–Stokes solvers.

Nomenclature

C_d	=	drag coefficient, $D/\frac{1}{2}\rho u^2$, where D is drag
C_l	=	lift coefficient, $L/\frac{1}{2}\rho u^2$, where L is lift
$\boldsymbol{c}_i$, $c_{i,\alpha}$	=	particle velocity vector and its component
$\tilde{\boldsymbol{c}}_i$, $\tilde{c}_{i,\alpha}$	=	contravariant velocity vector of the particle velocity and its component
f_i	=	distribution function
$f_i^{(\mathrm{eq})}$	=	equilibrium distribution function
f_i^*	=	postcollision distribution function
p	=	pressure
Re	=	Reynolds number
Re_{eff}	=	effective Reynolds number
t	=	time
$\boldsymbol{u}$, u_α	=	velocity vector of the flow and its component
w_i	=	weight function
$\boldsymbol{x}$	=	coordinates on physical plane
Δt	=	time incrementation
$\Delta\xi_{\mathrm{up},i}$	=	upwind point
$\delta_{\alpha\beta}$	=	Kronecker delta
ξ	=	coordinates on computational plane
ρ	=	density of the flow
ω	=	relaxation parameter
ω_{eff}	=	effective relaxation parameter

Presented as Paper 2004-224 at the AIAA 42nd Aerospace Sciences Meeting, Reno, NV, 5–8 January 2004; received 12 January 2004; revision received 25 March 2005; accepted for publication 28 March 2005.

*Researcher, Computational Aerodynamics and Optimization Team, Information Technology Center, Institute of Space Technology and Aeronautics, 7-44-1, Jindaiji Higashi-machi, Chofu. Member AIAA.

†Associate Professor, Department of Advanced Energy, Division of Transdisciplinary Sciences, Graduate School of Frontier Sciences, 7-3-1 Hongo, Bunkyo-ku. Senior Member AIAA.

‡Chief Manager, Administration Office, Information Technology Center, Institute of Space Technology and Aeronautics, 7-44-1, Jindaiji Higashi-machi, Chofu.

§Senior Researcher, Information Technology Center, Institute of Space Technology and Aeronautics, 7-44-1, Jindaiji Higashi-machi, Chofu.

Introduction

THE lattice Boltzmann method (LBM) has been proven to be a promising method in simulating incompressible flow, porous-media flow, and multiphase flow.[1] Because various modifications have been applied to LBM, the accuracy and the efficiency of the simulation have improved compared with the early stage of its development.

It is important to reduce the computational time to use LBM as a practical computational fluid dynamics tool. However, because the grid used in the standard LBM [commonly referred to as the lattice Bhatnagar–Gross–Krook (LBGK) model] is restricted to an orthogonal grid with equal spacing, the calculation for high-Reynolds-number flow with sufficient spatial accuracy requires more computer resources compared with the traditional Navier–Stokes solvers on a nonuniform mesh. Recently, many studies have been dedicated to the extension of the LBM on a nonuniform mesh. The strategies are classified into two groups. The first type is to patch the fine orthogonal grid only to the region where high resolution is required. The adaptive mesh refinement (AMR) technique[2] or composite grid system[3] used for Navier–Stokes solvers are applied to the LBM. Although the grid spacing is different between the grids, the algorithm applied to the each grid is exactly the same as LBGK. A special treatment is implemented only to the boundary of the grids where the exchange of values between the grids is necessary. The second strategy type is to use body-fitted grids, and this has been formulated by many authors.[4,5] With the use of these methods, flow around various configurations can be solved. Among these methods, interpolation supplemented LBM (ISLBM)[4] and the characteristic Galerkin finite element method for the discrete Boltzmann equation (see Ref. 5) seem to give results without excessive numerical dissipation.

In this paper, flow around an airfoil is calculated using LBM on generalized coordinates. The numerical method used in this study is based on the idea of ISLBM and is extended to a more generalized form by the authors.[6] Because the transformation between a physical plane and a computational plane must be described by an analytical function for ISLBM, a generalization of ISLBM is necessary to calculate on an arbitrary structured grid. Also, the present method is combined with a turbulence model to calculate high-Reynolds-number flows.

This paper is organized as follows. The next section describes the numerical methods used. Starting from the LBGK model,

a generalization of ISLBM to arbitrary structured grids is introduced. It is the generalized form of interpolation supplemented LBM (GILBM). The definition of boundary conditions and a turbulence model is also described. The next section presents the computational results and comparison with experimental data. The final section contains the conclusion. All of the descriptions made in this paper are for a two-dimensional plane.

Numerical Method

LBM on Orthogonal Grid System

The LBM describes flows by the collision and advection calculation of distribution functions as follows. The two-dimensional nine-velocity (2D9V) model is used in the present calculations. The governing equation of the LBM, the lattice Boltzmann equation (LBE), is

$$f_i(\boldsymbol{x} + \boldsymbol{c}_i\Delta t, t + \Delta t) - f_i(\boldsymbol{x}, t) = -(1/\omega)\left[f_i(\boldsymbol{x}, t) - f_i^{(\mathrm{eq})}(\boldsymbol{x}, t)\right] \tag{1}$$

where $i = 0, 1, 2, \ldots, 8$. The variables f_i and $f_i^{(\mathrm{eq})}$ are the distribution function and the equilibrium distribution function corresponding to the discrete velocity vector $\boldsymbol{c}_i$, respectively. The value Δt is the time step and ω is the relaxation time. The right- and left-hand sides of Eq. (1) correspond to the collision and the advection terms, respectively. Thus, Eq. (1) can be divided into two phases.

Collision term:

$$f_i^*(\boldsymbol{x}, t) = -(1/\omega)\left[f_i(\boldsymbol{x}, t) - f_i^{(\mathrm{eq})}(\boldsymbol{x}, t)\right] \tag{2}$$

Advection term:

$$f_i(\boldsymbol{x}, t + \Delta t) = f_i^*(\boldsymbol{x} - \boldsymbol{c}_i\Delta t, t) \tag{3}$$

The discrete velocity vector is defined as

$$[\boldsymbol{c}_0, \boldsymbol{c}_1, \boldsymbol{c}_2, \boldsymbol{c}_3, \boldsymbol{c}_4, \boldsymbol{c}_5, \boldsymbol{c}_6, \boldsymbol{c}_7, \boldsymbol{c}_8] = c\begin{bmatrix} 0 & 1 & 0 & -1 & 0 & 1 & -1 & -1 & 1 \\ 0 & 0 & 1 & 0 & -1 & 1 & 1 & -1 & -1 \end{bmatrix} \tag{4}$$

and the equilibrium distribution function is defined as

$$f_i^{(\mathrm{eq})}(\boldsymbol{x}, t) = w_i\rho\left[1 + \frac{3c_{i,\alpha}u_\alpha}{c^2} + \frac{9(c_{i,\alpha}u_\alpha)^2}{2c^4} - \frac{3u^2}{2c^2}\right] \tag{5}$$

with $w_0 = 4/9$, $w_1 = \cdots = w_4 = 1/9$, and $w_5 = \cdots = w_8 = 1/36$ for the 2D9V model.

The macroscopic variables such as density and velocity are obtained from integrating the moment of the distribution functions over the velocity plane as

$$\rho = \sum_i f_i, \qquad \rho\boldsymbol{u} = \sum_i f_i\boldsymbol{c}_i \tag{6}$$

When the Chapman–Enskog expansion is applied to the governing equation, the relation between the LBE Eq. (1) and the Navier–Stokes equations is obtained. The relationship between the relaxation time ω and the Reynolds number can be derived as

$$Re = 6/(2\omega - 1)\Delta t c^2 \tag{7}$$

and the pressure is given as $p = \rho c^2/3$.

GILBM

In this section, the LBM model for generalized coordinates is introduced based on the idea of ISLBM.[4] The physical plane $\boldsymbol{x}$ is transformed into a computational plane described by $\boldsymbol{\xi}$. Equations (2) and (3) are transformed into generalized coordinates as follows. The collision term on generalized coordinates is described as

$$f_i^*(\boldsymbol{\xi}, t) = -(1/\omega)\left[f_i(\boldsymbol{\xi}, t) - f_i^{(\mathrm{eq})}(\boldsymbol{\xi}, t)\right] \tag{8}$$

where ω, $f_i^{(\mathrm{eq})}(\boldsymbol{\xi}, t)$, and $f_i^*(\boldsymbol{\xi}, t)$ correspond to the relaxation time, the equilibrium distribution function, and the postcollision distribution function, respectively. The advection term is solved as

$$f_i(\boldsymbol{\xi}, t + \Delta t) = f_i^*(\boldsymbol{\xi} - \Delta\boldsymbol{\xi}_{\mathrm{up},i}, t) \tag{9}$$

where

$$\Delta\boldsymbol{\xi}_{\mathrm{up},i} = (\Delta\xi_{\mathrm{up}}, \Delta\eta_{\mathrm{up}}) = \int_0^{\Delta t} \mathrm{d}\boldsymbol{\xi} = \int_0^{\Delta t} \tilde{\boldsymbol{c}}_i\,\mathrm{d}t \tag{10}$$

This is the time integration of the contravariant velocity. A two-step Runge–Kutta method is used for the integration of Eq. (10) to maintain numerical accuracy in the highly clustered grid region. When the metrics and the discrete velocity $c_{i,\beta}$ are used, the contravariant velocity $\tilde{c}_{i,\alpha}$ is obtained as

$$c_{i\alpha} = c_{i\beta}\frac{\partial\xi_\alpha}{\partial x_\beta} \tag{11}$$

where the summation convention is used for the subscript α, β. The right-hand side of Eq. (9) should be calculated using a second-order upwind multidimensional interpolation.[4] When the contravariant velocity is introduced, the advection term is calculated in the computational space, and the grid is not restricted to any specific grid system for LBM, such as for isotropic grids.

Boundary Conditions of GILBM on Generalized Coordinates

In this study, suitable wall boundary conditions for the generalized coordinates are obtained based on the idea of the incompressible Navier–Stokes solvers (see Ref. 6). The wall boundary condition for the incompressible Navier–Stokes solvers is defined as follows. Because the normal gradient of the pressure vanishes at the wall boundary, pressure on the wall, $p_{j=0}$, is extrapolated from the node in the computational domain next to the wall boundary node as $p_{j=0} = p_{j=1}$. In LBM, a similar expression for density is obtained as $\rho_{j=0} = \rho_{j=1}$. The flow velocity at the wall is given as the wall velocity.

From the boundary condition of the macroscopic variables (ρ, u, and v), the boundary condition of the distribution function is calculated. If we assume $f_i \cong f_i^{(\mathrm{eq})}$, the distribution function can be calculated using Eq. (5). However, this assumption is not accurate enough because the viscosity effect appears in the first order of the nonequilibrium term. The distribution function is estimated to the first order of nonequilibrium using the Chapman–Enskog expansion as

$$f_i \cong f_i^{(\mathrm{eq})} + f_i^{(1)} = f_i^{(\mathrm{eq})}\left[1 - \omega\Delta t\left(\frac{3U_{i\alpha}U_{i\beta}}{c^2} - \delta_{\alpha\beta}\right)\frac{\partial u_\alpha}{\partial x_\beta}\right] \tag{12}$$

where $U_{i,\alpha} = c_{i,\alpha} - u_\alpha$.

Turbulence Modeling

For high-Reynolds-number flows, which often appear in practical engineering problems, a direct approach is not realistic because of limited computational resources. To include phenomena due to scales smaller than the grid size, a turbulence model developed for the Navier–Stokes equations is combined with the GILBM.

Combination of the LBM and turbulence models was discussed by Teixeira.[7] Various turbulence models proposed for the Navier–Stokes equations, such as algebraic models, two-equation models, etc., are applied to LBM. Following the procedure proposed by Teixeira, the Baldwin–Lomax turbulence model (see Ref. 8) was implemented in this study to demonstrate the capability for the present GILBM to calculate turbulent flows. The only change to GILBM is the calculation of the relaxation time, due to the contribution of the eddy viscosity ν_T to the total viscosity ν. Thus, the effect of relaxation time becomes a function of the local flow quantities,

$$\omega_{\mathrm{eff}} = 3\Big/Re_{\mathrm{eff}}c^2\Delta t + \tfrac{1}{2} \tag{13}$$

where $1/Re_{\mathrm{eff}} = 1/Re + \nu_T/(\rho_0 U_0 L)$.

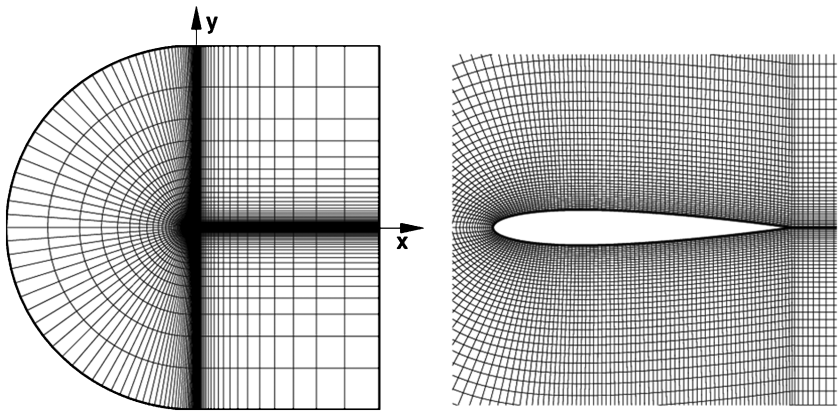

Fig. 1 Body-fitted grid used in NACA0012 airfoil simulations.

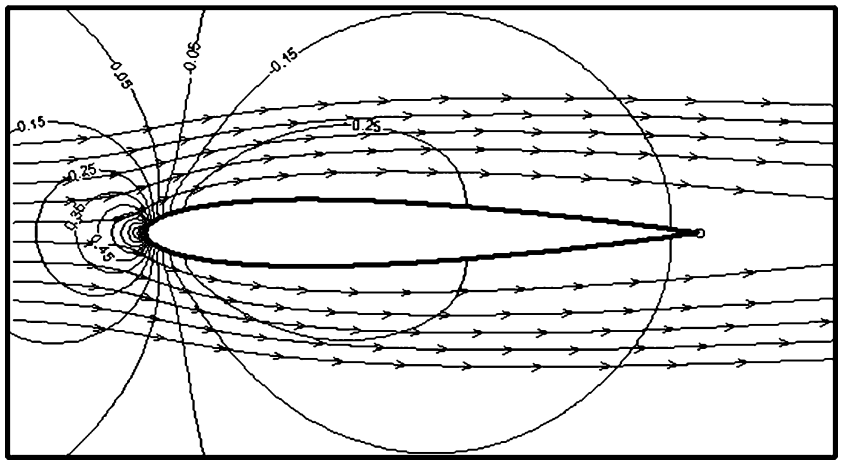

Fig. 2 Pressure contour and streamlines around NACA0012 at $Re = 500$.

Numerical Results

Code Validation of GILBM

The first example is the flow around a NACA0012 airfoil with a relatively small Reynolds number. The shape of the airfoil is symmetric, and the wing thickness is 12% of the chord length. Because an airfoil is a streamlined shape, a wall boundary condition formulated on body-fitted coordinates is desirable to obtain the aerodynamic coefficients accurately. The present method, with the Chapman–Enskog boundary condition on the wall, has the potential to yield more accurate computational results than those obtained using orthogonal grids. The Reynolds number is based on the macroscopic freestream velocity and the chord length of the airfoil. A body-fitted grid (C grid) is used in the present simulations, as shown in Fig. 1. The grid is formed by the transfinite interpolation method. With the chord length as a unit length, the computational domain consists of a half-circle of radius 20 in front of the airfoil and a rectangle of dimension 21×40. The outer boundary uses a nonreflecting-type boundary condition. The ratio of macroscopic velocity of the far field to the particle velocity is defined as $U/c = 0.1$. The calculation is performed at laminar flow conditions with $Re = 500$ and an angle of attack (AOA) of 0 deg. Figure 2 shows the pressure contours and streamlines obtained by the present method. A symmetric flow pattern is observed. Figure 3 shows the pressure coefficient distribution along the surface of the airfoil. Results obtained by CFL3D and PowerFLOW[9] are also plotted in Fig. 3. CFL3D is a Navier–Stokes solver using the finite volume formulation on generalized coordinates, and PowerFLOW is a commercially available LBM solver using orthogonal grids with the AMR technique. The pressure distribution agrees well with the CFL3D result. Figure 4 indicates the velocity profile of the boundary layer at $x = 0.00$, 0.25, 0.50, 0.75, and 1.00 of the chord length (Fig. 4a), respectively. At $x = 0.00$, the present calculated results are consistent with the other two simulations. As the location moves to the downstream side, the

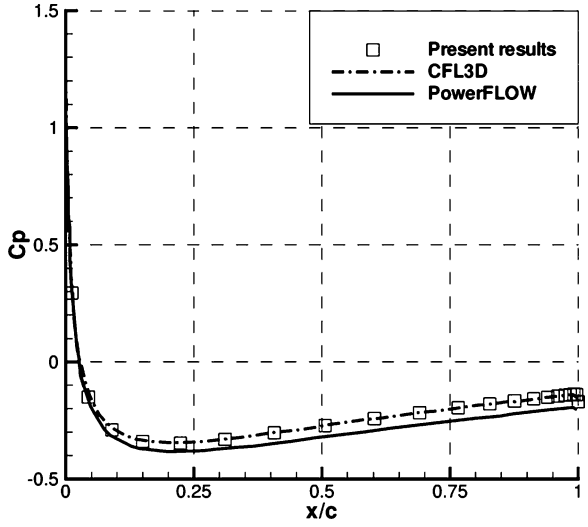

Fig. 3 Pressure distribution along surface of NACA0012.

result obtained by PowerFLOW becomes different from the other two. Although a sufficiently small grid was used in the PowerFLOW simulation, the boundary layer is not accurately resolved. The difference is significant for the y-direction velocity component V in Fig. 4f (at $x = 1.00$). On the other hand, the method outlined here produces pressure and velocity profiles very similar to those of CFL3D.

The dependence of the aerodynamic coefficients on the grid resolution and the minimum grid spacing is studied in detail, as shown in Table 1. The aerodynamic coefficients are compared with those of the other two methods. Also lift coefficient C_l shows excellent

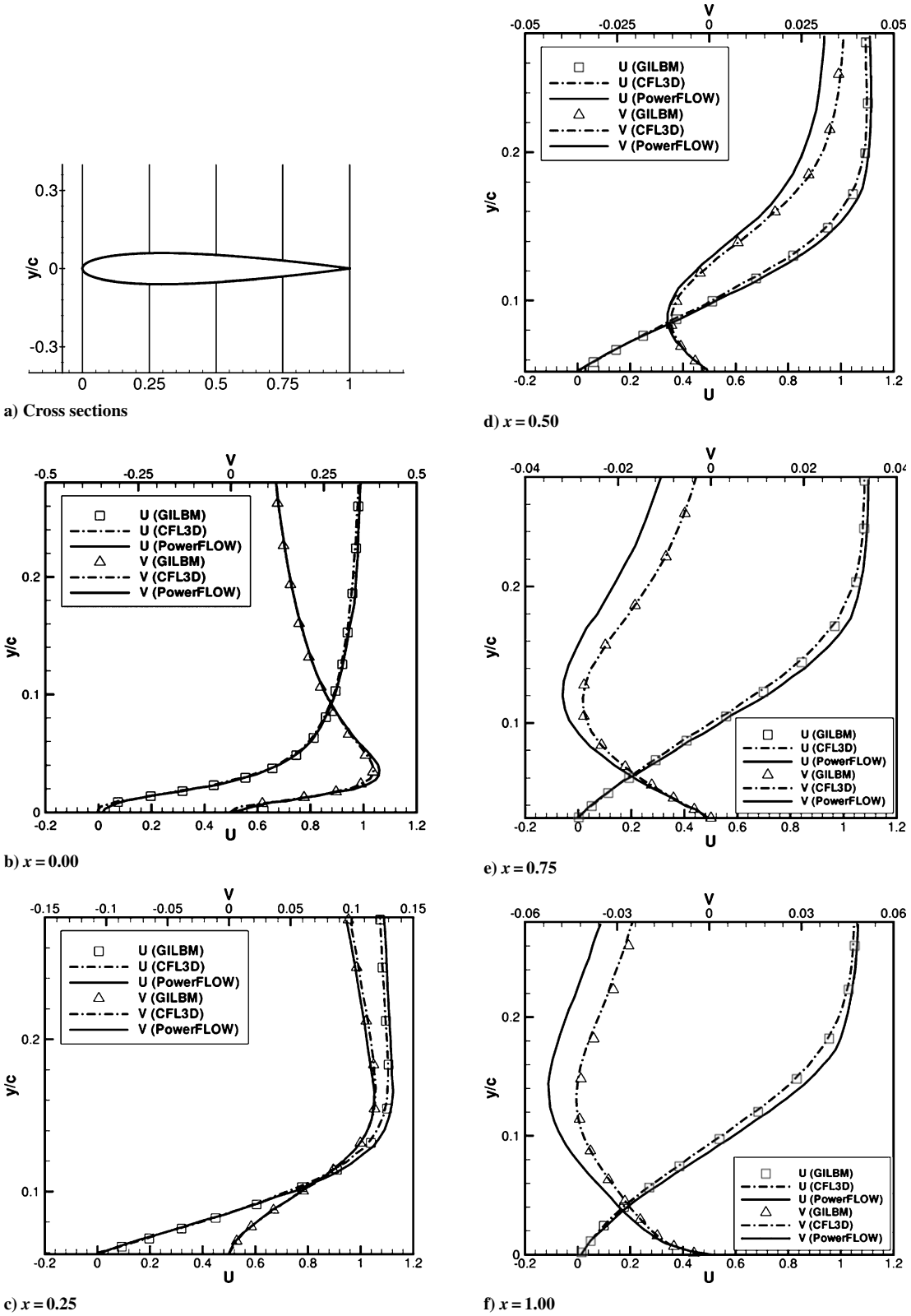

Fig. 4 Velocity profile of NACA0012 at various cross sections x.

symmetry of the calculation. The value of the drag coefficient C_d obtained from the present method using the highest-resolution grid is about 0.9% smaller than that of CFL3D. As the resolution becomes higher, the drag coefficient converges to a value close to the results obtained by CFL3D.

High-Reynolds-Number Simulation

In this section, we present flows around a NACA0012 airfoil at Reynolds numbers of 5×10^5 and 6.6×10^5. The calculation at the lower Reynolds number is performed to compare the results with the Navier–Stokes solution obtained by CFL3D (see Refs. 9 and 10). CFL3D uses the Spalart–Allmaras turbulence model. The calculation at the higher Reynolds number is performed to compare the results with experimental data. Also, results obtained by the latest version of PowerFLOW, PowerFLOW 3.2, is available for both Reynolds numbers. PowerFLOW 3.2 is based on the extension of the two-equation turbulence model originally derived from the renormalized group method.

The first two calculations were performed for $Re = 5 \times 10^5$ and AOA = 7 deg to show the ability of the present method to calculate the flow with the turbulence model. A body-fitted grid (C grid) with grid resolution of 257×65 is used in the present simulations. One calculation is performed assuming laminar flows; the other uses the Baldwin–Lomax turbulence model. Figures 5a and 5b show the pressure distribution and streamlines near the wing calculated with and without the turbulence model, respectively. Generally speaking, separation around the wing is suppressed when the turbulence model is used. The present calculation by GILBM shows a similar tendency; the flow separation over the wing disappears when the turbulence model is used. Consequently, it is expected that the turbulence model is adequately combined with GILBM. This can be confirmed by the pressure coefficient distribution along the surface of the airfoil as shown in Fig. 6. The present result shows excellent agreement with the CFL3D solution. Table 2 summarizes the aerodynamic coefficients for different calculation methods for $Re = 5 \times 10^5$ and AOA = 7 deg. The present calculation with Baldwin–Lomax model gives results almost identical to those of CFL3D. Without the turbulence model, the aerodynamic coefficients oscillate due to flow separation. On the other hand, PowerFLOW 3.2 overpredicts the drag coefficient.

Second, to provide a comparison with experimental results, flow simulations at $Re = 6.6 \times 10^5$ are performed for a range of AOA from 0 up to 16 deg. Figure 7 shows the C_l vs AOA and C_l vs C_d. Present results provide reasonable agreement before the separation occurs. The lift slope and drag coefficient agree with the experimental data. Also the dip in C_l due to the separation is predicted by the present method. The experimentally predicted stall angle for a NACA0012 airfoil at $Re = 10^5$–10^6 is around 13 deg. The stall angle predicted by the present simulation is around 10 deg, which is smaller than that of the experiment. The difference is not caused

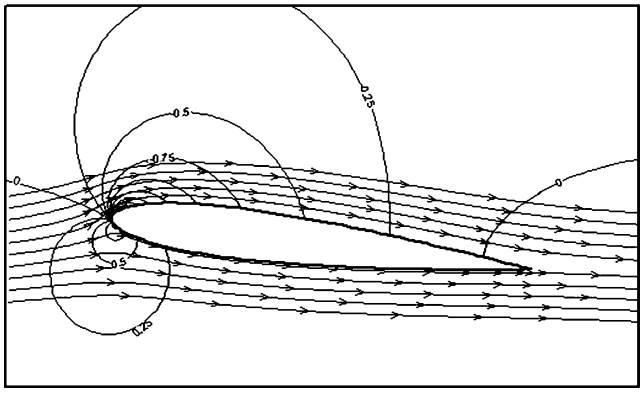

a)

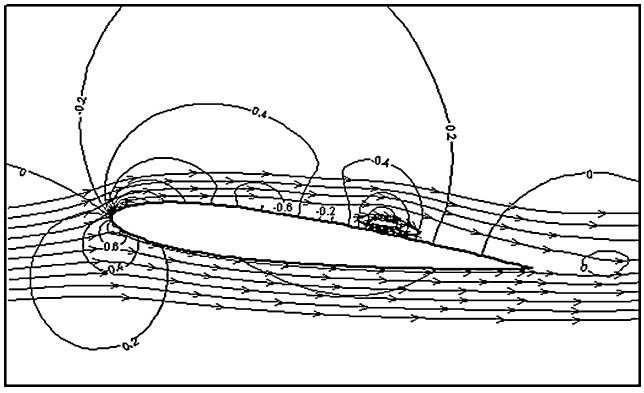

b)

Fig. 5 Pressure contour and instantaneous streamline around NACA0012 airfoil at $Re = 5 \times 10^5$: a) with turbulence model and b) without turbulence model.

Table 1 Grid resolution dependency

Resolution (on wing)	$\Delta x_{\min}$	C_d	C_l
	GILBM		
257×65 (173)	$4.5e{-3}$	0.1682	$1.0e{-13}$
373×141 (251)	$4.5e{-3}$	0.1672	$1.0e{-13}$
257×65 (173)	$4.5e{-4}$	0.1736	$1.0e{-13}$
373×141 (251)	$4.5e{-4}$	0.1725	$1.0e{-13}$
	PowerFLOW		
159,060 (828)	$1.2e{-3}$	0.1717	$0.227e{-3}$
418,800 (1275)	$7.8e{-4}$	0.1807	$-0.211e{-3}$
	CFL3D		
257×65	——	0.1762	$0.115e{-6}$
373×141	$1.2e{-4}$	0.1741	$0.538e{-5}$

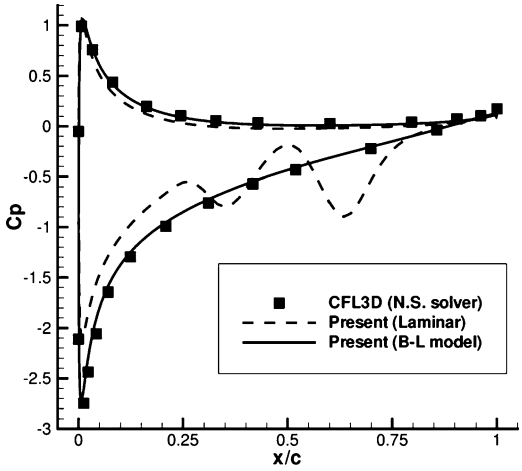

Fig. 6 C_p distribution along the chord of NACA0012 at $Re = 5 \times 10^5$.

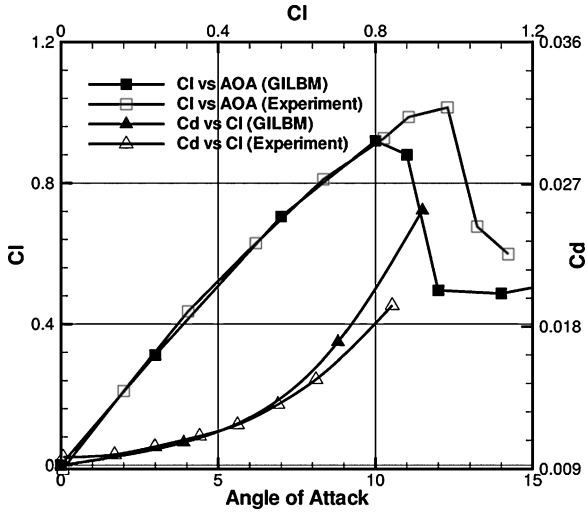

Fig. 7 C_l vs AOA and C_l vs C_d.

Table 2 Aerodynamic coefficients for flow around NACA0012 airfoil at $Re = 5 \times 10^5$ and AOA = 7 deg

Methods	C_d	C_l	Grid size
Present (Baldwin–Lomax model)	0.0177	0.6979	257×65 (16,705 cells)
Present (laminar)	0.03×0.015	0.55×0.11	257×65 (16,705 cells)
CFL3D (Spalart–Allmaras model)	0.0157	0.7449	257×65 (16,705 cells)
PowerFLOW 3.2	0.028	0.63	800,000 cells

by the LBM itself because the effect of minimum grid size and the choice of turbulence model is considered to be more significant. Further studies are required regarding this issue.

Conclusions

An LBM for generalized coordinates, GILBM, is proposed to calculate high-Reynolds-number flows efficiently. Additionally, numerical techniques to enhance the accuracy and efficiency of the GILBM are developed as follows:

1) A new wall boundary condition for generalized coordinates is introduced. It is necessary for the accurate prediction of the drag coefficient.

2) The GILBM and the Baldwin–Lomax turbulence model are combined. This is necessary for high-Reynolds-number-flow analysis.

When the present code is used, flows around an airfoil are calculated efficiently and the results are consistent with previous Navier–Stokes solutions. In particular, the combination of GILBM and the Baldwin–Lomax model gives better results compared with the laminar LBM calculation for the present airfoil simulations at high Reynolds numbers. Also the results are in good agreement with the experimental data. With the same grid resolution, GILBM can solve high-Reynolds-number flows as accurately as traditional Navier–Stokes solvers.

Acknowledgments

This work was done as a joint research project with the National Aerospace Laboratory of Japan. The vector-parallel supercomputer, Numerical Wind Tunnel, was used for some of the calculations.

References

[1]Chen, S., and Doolen, G., "Lattice Boltzmann Method for Fluid Flows," *Annual Review of Fluid Mechanics*, Vol. 161, 1998, pp. 329–364.

[2]Fillipova, O., Succi, S., Mazzocco, F., Arrighetti, C., Bella, G., and Hanel, D., "Multiscale Lattice Boltzmann Schemes with Turbulence Modeling," *Journal of Computational Physics*, Vol. 170, No. 2, 2001, pp. 812–829.

[3]Lin, C.-L., and Lai, Y. G., "Lattice Boltzmann Method on Composite Grids," *Physical Review E*, Vol. 62, No. 2, 2000, pp. 2219–2225.

[4]He, X., and Doolen, G., "Lattice Boltzmann Method on Curvilinear Coordinate System: Flow Around a Circular Cylinder," *Journal of Computational Physics*, Vol. 134, No. 2, 1997, pp. 306–315.

[5]Lee, T., and Lin, C.-L., "A Characteristic Galerkin Method for Discrete Boltzmann Equation," *Journal of Computational Physics*, Vol. 171, No. 1, 2001, pp. 336–356.

[6]Imamura, T., "Incompressible Flow Simulation Using Generalized Interpolation-Based Lattice Boltzmann Method," Ph.D. Dissertation, Dept. of Aeronautics and Astronautics, Faculty of Engineering, Tokyo Univ., Tokyo, 2003.

[7]Teixeira, C. M., "Incorporating Turbulence Models into the Lattice-Boltzmann Method," *International Journal of Modern Physics C*, Vol. 9, No. 8, 1998, pp. 1159–1175.

[8]Wilcox, D. C., *Turbulence Modeling for CFD*, 2nd ed., DCW Industries, La Canada, CA, 1998, pp. 76–79.

[9]Lockard, D. P., Luo, L., Milder, S. D., and Singer, B. A., "Evaluation of PowerFLOW for Aerodynamic Applications," *Journal of Statistical Physics*, Vol. 107, Nos. 1–2, 2002, pp. 423–478.

[10]Shock, R. A., Mallick, S., Chen, H., Yakhot, V., and Zhang, R., "Recent Results on Two-Dimensional Airfoils Using a Lattice Boltzmann-Based Algorithm," *Journal of Aircraft*, Vol. 39, No. 3, 2002, pp. 434–439.

C. Kaplan
Associate Editor